Processing Methods of Ultrathin Poly(ϵ-caprolactone) Films for Tissue Engineering Applications

Kay Siang Tiaw,[†,‡] Swee Hin Teoh,*[,†] Ran Chen,[†] and Ming Hui Hong[‡,§]

*Centre for Biomedical Materials Applications and Technology (BIOMAT), Department of Mechanical Engineering, National University of Singapore, 10 Kent Ridge Crescent, 119260 Singapore, Optical Materials and Systems Division, A*STAR Data Storage Institute (DSI), 5 Engineering Drive 1, 117608 Singapore, and Department of Electrical and Computer Engineering, National University of Singapore, 10 Kent Ridge Crescent, 119260 Singapore*

Received August 28, 2006; Revised Manuscript Received December 25, 2006

Ultrathin poly(ϵ-caprolactone) (PCL) films were fabricated through biaxially drawn films made from three different methods, namely, spin casting, 2-roll milling, and solution casting. Biaxial drawn spin cast films yield thickness of 1.2 μm which is 9 and 12 times thinner that 2-roll mill and solvent cast films, respectively. The films fabricated were found to exhibit different drawing ratios. 2-roll mill film exhibits the highest drawing ratio of 4 × 4 while spin cast films can only draw up to a ratio of 2 × 2. The morphology of the films, studied using a polarized microscope and atomic force microscope, showed fine fibrillar networks of different thicknesses. Biaxially drawn 2-roll mill and solvent cast films showed thicker fibrils as compared to those for the spin cast films. Such a difference can be attributed to larger spherulites caused by slower cooling rates during melt pressing for both 2-roll mill and solvent cast films and smaller spherulites because of fast cooling during evaporation for spin cast films. Thermal analysis through differential scanning calorimetry revealed a slight increase in the peak-melting temperature after biaxial drawing. A drop in percentage crystallinity was also noted. The result of the water vapor transmission rate (WVTR) was found to be dependent on fabrication techniques that determine the spherulites formation. It was also found that the WVTR was inversely proportional to the thickness of the films. Tensile strength and modulus of the films showed significant improvements after biaxial stretching. By identifying the unique strengths of each individual PCL film produced via different techniques, it is possible to apply to different areas of membrane tissue engineering such as dermatology, ophthalmology, vascular graft engineering, and soft tissue regeneration.

Introduction

Development and fabrication of thin polymer films through a variety of methods has spawned wide applications from industry to biomedical sciences. Although there are different methods in the fabrication of thin polymeric films, each method brings about different properties and characteristics to the films in terms of strength, ductility, and permeability. Extrusion, calendaring, and blowing are the common industrial methods for fabricating polymer sheets and thin films[1,2] of thickness ranging from tens to hundreds of micrometers. These methods usually produce low to moderate level of chain orientation and are only suitable for low to moderate load-bearing applications. There is also a limitation to which the thickness of the films can reach at its minimum through the more readily methods as mentioned above. However, such limitation can be overcome by physically drawing the films to give thinner films and at the same time improve the tensile strength and modulus because of the induced orientation of the fibrils.[3] Uniaxial drawing can improve its physical properties only along its drawing direction and the use of uniaxial drawn films have to be exercised with caution as wrong direction in the load applied may lead to failure. Sequential or simultaneous biaxial drawing[4−12] have been carried out extensively as the physical properties are improved in both the longitudinal and lateral directions. Such superior quality of biaxial drawn films over uniaxial drawn films is the reason for the extensive use of biaxial drawn films for packaging applications.

With increasing interest in the use of biodegradable polymer in the area of biomedical science, extensive research has been carried out. Biodegradable polymers include poly(lactide), poly(glycolide), poly(ethylene glycolide), and poly(ϵ-caprolactone). These biodegradable materials are suitable for pharmaceutical products such as wound dressings which require durability, stress resistance, flexibility, and good elasticity. The surface chemistry of the biodegradable polymers can also be modified to provide good and uniform adherence and to conform to the wound topography to prevent accumulation of air or liquid pockets. Besides good adherence, it must also provide a barrier to prevent infections that can be caused by bacteria penetration. The water vapor permeability is also an important aspect to consider, such as to prevent fluid accumulation under the dressing while at the same time maintaining an optimum moist condition.[13−14] For the criteria to minimize adverse long-term host-tissue response to foreign material, thin membrane structure needs to be considered. For membrane tissue engineering in ophthalmology, dermatology and even vascular graft engineering, polymer films are seen as favorable matrixes because less material is involved and hence will invoke minimal adverse host-tissue response. Also, the use of such films as stromal substitutes are

* To whom correspondence should be addressed. Tel: +65-6874-4605; fax: +65-67791459; e-mail address: mpetsh@nus.edu.sg.

† Department of Mechanical Engineering, National University of Singapore.

‡ A*STAR Data Storage Institute.

§ Department of Electrical and Computer Engineering, National University of Singapore.

10.1021/bm060832a CCC: $37.00
Published on Web 02/03/2007

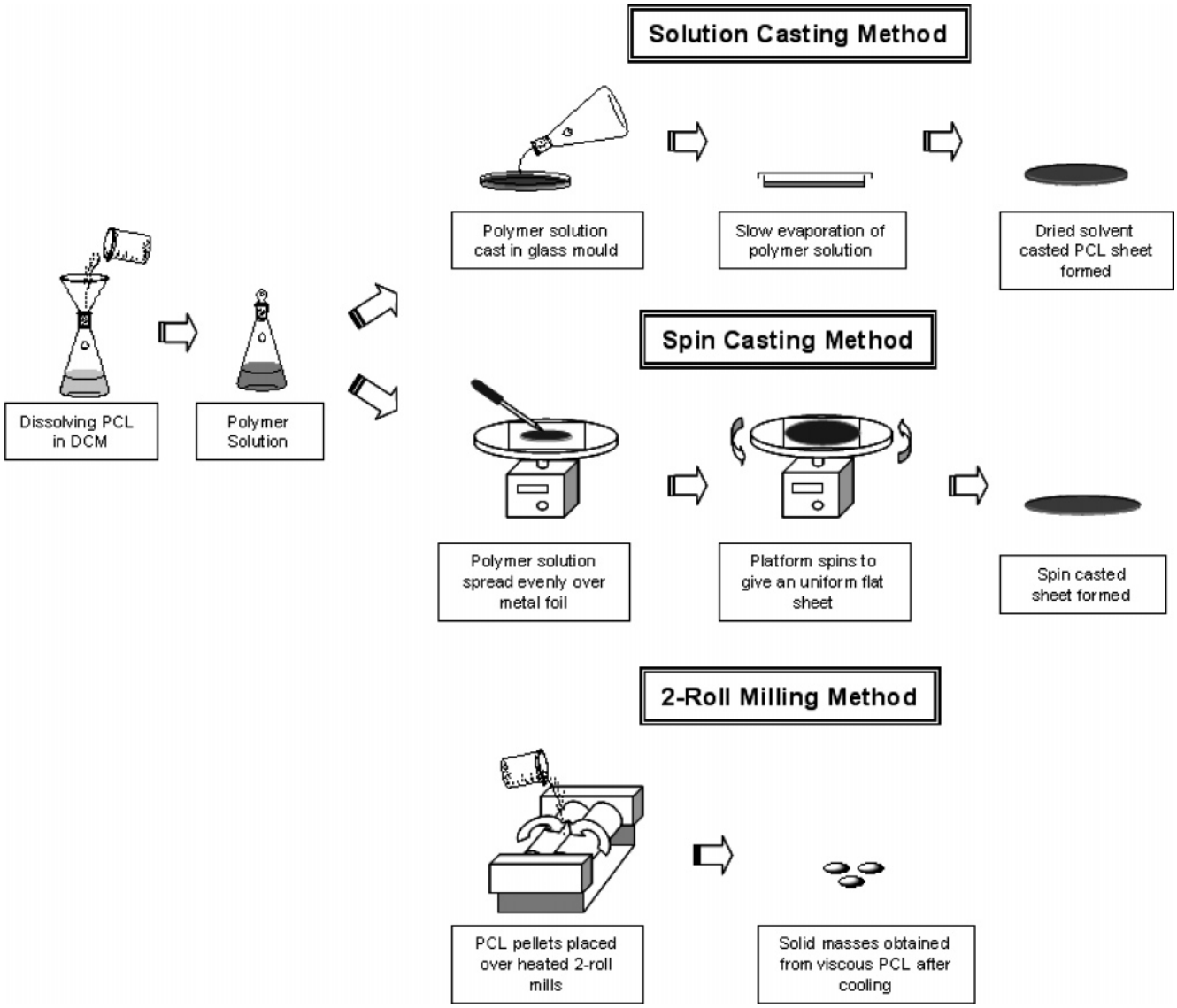

Figure 1. Schematic drawing showing the stages of initial preparation of PCL thin film using methods of solvent casting, 2-roll milling, and spin casting.

found to be able to support cell growth and this is especially an important development as this would mean that the use of allogenic biological material as substrates can be completely phased out, hence overcoming problems of disease transmission or allograft rejection.[15−16]

Microthin films of 10-μm thick through biaxial drawing of poly(ϵ-caprolactone) (PCL) films have been developed successfully by Teoh's group[4] and subsequent tests have proven that PCL thin films are suitable for membrane tissue engineering.[17−19] The excellent mechanical properties of PCL thin films also allow easy handling for in-vitro and in-vivo research work. Further treatment of the PCL films were also carried out to enhance cell-biomaterial interaction.[8,9,18,20]

It will be a challenge in the area of membrane tissue engineering if the thickness of thin polymer films can be achieved at sub-micrometer thickness with reasonable mechanical properties. Thin films in the scale of nanometer thickness have been successfully achieved using spin cast technique.[21,22] However, such method produce films which are very strongly adhered to a substrate surface such as glass or silicon. It is virtually not possible to remove the thin films from the substrate surface at such nanometer scale thickness. This paper reports on the ways of achieving ultrathin PCL films in region of sub-micrometer thickness through a two-step process. The polymer solution was first spin cast to achieve films with approximate thickness of 6.3 ± 1.4 μm. The spin cast films were then subjected to biaxial drawing to obtain ultrathin PCL films of 1.2 ± 0.5 μm thick. PCL films fabricated through 2-roll milling and standard solution casting followed by biaxially drawn were also compared. The physical, mechanical, water moisture permeability, and thermal characteristics of the biaxial drawn and undrawn films were investigated and discussed.

Experimental Section

Materials. The PCL pellets used were purchased from Sigma-Aldrich. They have a density of 1.145 g/cm^3 of number-average molecular weight (M_n) of 80 000. The polydispersity of PCL as determined by gel permeation chromatography was 1.51. The glass-transition temperature and melting temperature of PCL are −60 °C and 60 °C, respectively. Since PCL has a low-glass-transition temperature, it exists in rubbery state at room temperature, which explains its excellent tensile-drawing ability.

Film Preparation. PCL ultrathin films were fabricated using three techniques, namely, solvent casting, 2-roll milling, and spin casting. The use of 2-roll mill does not require solvent whereas the other two

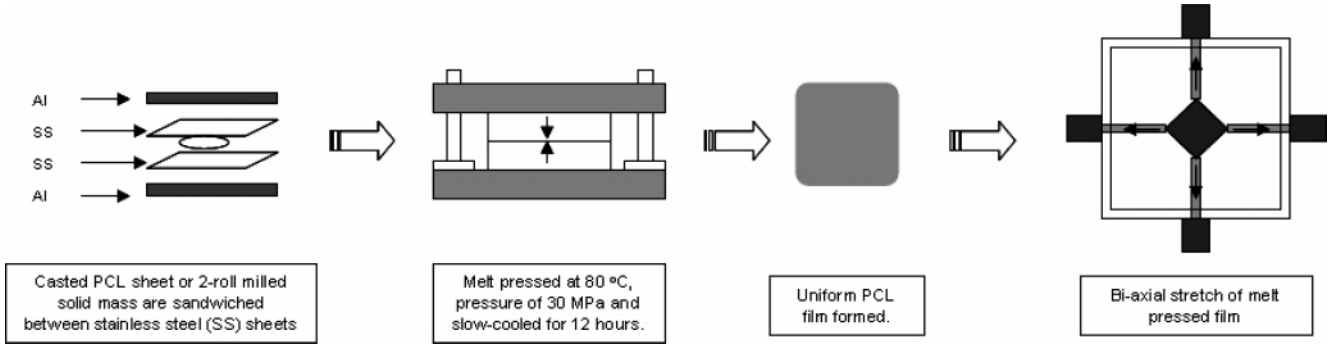

Figure 2. Stages of heat treatment and biaxial drawing.

methods require the solvent for the polymer solution to flow and evaporate into thin sheets. The initial steps of the film preparation are represented in Figure 1 and described as follows.

Solvent Casting. Polymer solution was prepared by dissolving PCL pellets in methylene chloride at a concentration of 3 wt % and casting over glass molds. A metal foil was placed on top of the molds to allow slow evaporation of the solvent. The solvent-casted films obtained were further dried in a vacuum oven at 40 °C to remove any remaining solvent. Solvent-casted films of thickness 120 μm can be uniformly achieved.

2-Roll Milling. PCL pellets were gradually fed in between the rolls, which were heated up to 80 °C with a rolling speed of 1 rpm. The pellets melted completely and formed a highly viscous liquid layer that adhered on the surface of the rolls. The layer of PCL was collected by using a blade to scrap off the viscous liquid from the rolls' surface and by allowing it to solidify into a uniform piece. The solid was next cut into smaller masses ready for melt pressing.

Spin Casting. This method of fabricating the PCL film evolved from the idea of a spin-coating machine for coating photoresist polymer in the semiconductor industry. A simple and effective spin cast device was self-developed by mounting a rotating platform to the rotor of a speed control motor. Polymer solution was then placed on the platform and was covered with a bell jar before the platform was set to spin at the desired rate of revolution. The initial preparation was similar to solvent casting where PCL pellets were dissolved in methylene chloride to give a polymer solution at a concentration of 3 wt %. An amount of 5 cm^3 of the solution was spread over an area of approximately 20 cm^2 on a metal sheet which was attached to a rotating platform. The platform was then rotated at a revolution of 500 rpm for 5 min. Uniformly spin cast PCL films of thickness approximately 6.3 ± 1.4 μm were produced and the spin cast films were next placed in a vacuum oven for similar reason.

Upon the completion of the initial preparation stages of the three methods, heat treatment and simultaneous biaxial drawing of the film followed, as shown in Figure 2. The solvent cast film, roll-mill mass, or spin-cast film was sandwiched between two aluminum foils and was melt-pressed at 80 °C and at a pressure of 30 MPa. After 10 min, the sandwiched film was allowed to slowly cool under pressure for 12 h. The melt-pressed film obtained was then preheated before being biaxially drawn in a temperature-controlled chamber at a temperature of 58 °C, which was just 2 °C below the melting point of PCL. After drawing, the film was annealed at the same temperature for a further 6 h. The thickness of the films produced by the three methods before and after being biaxial drawn is shown in Table 1.

Characterizations. The morphology of the PCL films was examined using a Nikon Optiphot-Pol Polarizing microscope. The optical images were captured using a Nikon Coolpix 4500 digital camera attached to the microscope with a Nikon Coolpix MDC lens mounted on the phototube. Fine details of the microstructures of the PCL film were examined using atomic force microscopy (Digital Instrument Nanoscope 111a AFM) over an area of 20 μm × 20 μm and 5 μm × 5 μm via tapping mode.

Table 1. Thickness of Nonbiaxially and Biaxially Drawn Films Produced by Different Methods

	mean film thickness (μm)	
method	nonbiaxiallly drawn	biaxially drawn
spin cast	6.3	1.2
2-roll mill	95.0	9.3
solvent cast		15.0

The thermal properties (peak temperature and enthalpy of fusion) of PCL films were studied using a Perkin-Elmer Pyris-6 Different Scanning Calorimeter (DSC). The instrument was calibrated with In and Zn standards. The PCL film samples were scanned from 20 °C to 80 °C at a heating rate of 5 °C/min under nitrogen atmosphere. The percentage crystallinity of the samples was estimated by comparing 100% crystalline PCL with enthalpy of fusion of 139.5 J/g.[23]

Permeability to water moisture of the films was determined by the water vapor transmission rate across the films. This experiment was carried out in accordance to ASTM E96-00 E. The films were wrapped around the opening of centrifuge tubes which were filled with 15 mL of deionized water and were almost 95% full and were left with about 5 mm of air gap. The opening of the tube has an area of 113 mm^2. An environment chamber (Contherm 5200 RHS, New Zealand) was used and the temperature and relative humidity of the chamber were set at 32 °C and 50%, respectively. Five samples for each specimen group were used to conduct the experiment. The experiment was conducted over a period of 21 days during which the mass of water loss was recorded.

The water vapor transmission rate (WVTR) was determined by the following equation:[24]

$$\mathrm{WVTR} = \frac{(G/t)}{A} = \frac{\mathrm{flux}}{\mathrm{area}}$$

where G, t, and A represent weight change (g), time during which G occurred (h), and the opening area of centrifuge tube (m^2), respectively. (G/t) is also known as the flux of the water vapor across the film thickness.

Tensile properties of the PCL films were determined using an Instron Universal tensile tester at standard room conditions. The samples were cut into strips of width measuring 10 mm and were mounted onto pneumatic grips. The grip separation was set at 30 mm and a testing speed of 5 mm/min was used. The thickness of the films was measured using an electronic length measuring equipment with an accuracy of 0.1 μm (Carycompar B Vertical comparator, V150) from TESA TECHNOLOGY.

The samples were subjected to tensile stress till break and stress−strain curves were plotted from the data generated. The modulus (E), ultimate tensile strength σ_{UTS}, and elongation (λ) were then subsequently extracted.

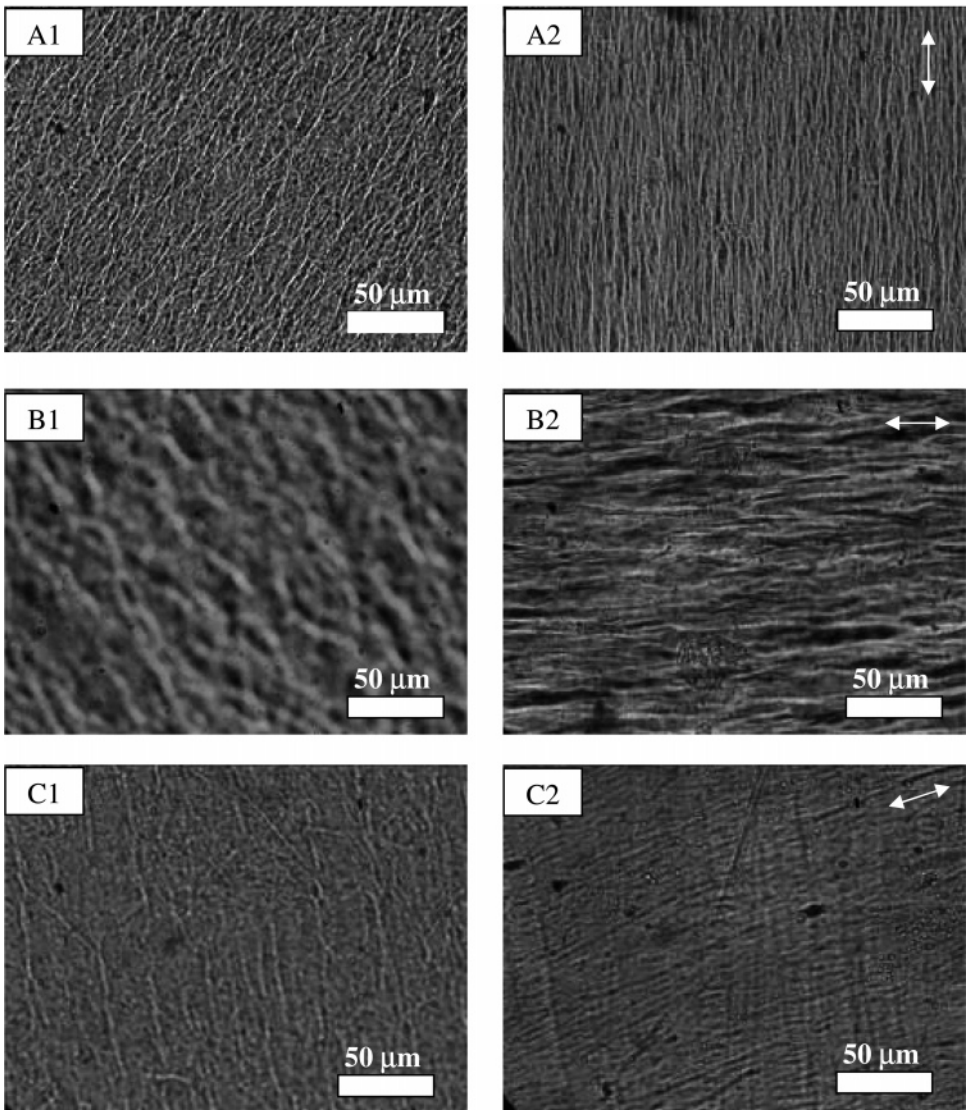

Figure 3. Morphology from polarizing microscope showing the different orientation of the fibrillar network of the biaxially drawn films of different fabrication methods (A: spin cast; B: 2-roll mill; C: solvent cast) at regions of center (1) and side (2).

Results and Discussion

Drawing Ability of Films. The films were drawn to their limit at near melting temperature of PCL. It has long been established that the limiting degree of drawing is dependent on the temperature at which the polymer was drawn.[6] It was found here that films produced by different techniques exhibit different drawing ratios at the same drawing temperature, as shown in Table 1. Before drawing, the thicknesses of heat-pressed films produced by 2-roll mill and solvent cast were approximately 95.0 μm while that of spin cast films were approximately 6.3 μm. Films produced using 2-roll mill had the largest drawing ratio of 4 $\times$ 4, followed by solvent cast of 3 $\times$ 3 and spin cast of 2 $\times$ 2.

One of the reasons for the difference in the drawing ratio between 2-roll mill and solvent cast films despite similar film thickness could be because the solvent used in solvent cast film may not be totally removed during evaporation. The remains of the solvent residing within the solvent cast film introduced defects such as small pores and thus could be the reason for its lower drawing ratio than 2-roll mill film. The three methods produce different microstructures (especially in fibrils thickness) of these PCL films, as shown in Figure 3. The thick fibrils of the biaxial drawn 2-roll mill film allowed a better drawing ratio as compared to the thinner fibrils of the biaxial drawn solvent cast films. Films produced by spin casting before drawing were 15 times thinner than that for solvent cast and 2-roll mill films. Although these films had a relatively low drawing ratio as compared to the rest, very thin films of thickness approximately 1.2 μm were successfully achieved.

The drawing ratio of the films could also be affected by their molecular weight M_n. It is known that polymer chain with a higher M_n has a higher tensile strength and elongation than one with a lower M_n. It was reported that for thermal degradation of PCL to take place, temperatures of 230 °C and 355 °C would be required for PCL with M_n of 1800 and 42 450, respectively.[25] For higher M_n of 80 000, thermal degradation takes place at even higher temperatures of up to 430 °C.[26−28] Hence, melt pressing at 80 °C should not trigger degradation to cause chain reduction to PCL. Therefore, the PCL films reported here that had previously undergone melt pressing way below the degradation temperature would not have resulted in any significant degradation.

Morphology. The polarized optical micrographs of the PCL films processed using different techniques are shown in Figure 3. This figure shows images of biaxially drawn films by methods of spin cast (A), 2-roll mill (B), and solvent cast (C) at regions

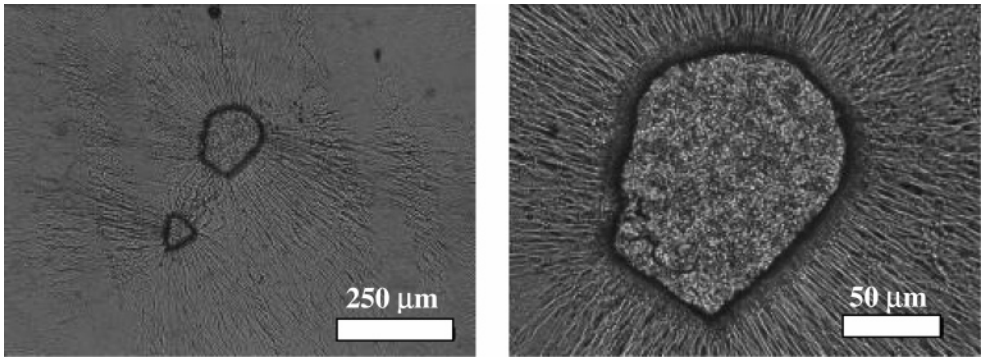

Figure 4. Morphology from polarizing microscope showing fibrils extending outward radially from the undrawn material of biaxially stretched spin cast PCL films at center region.

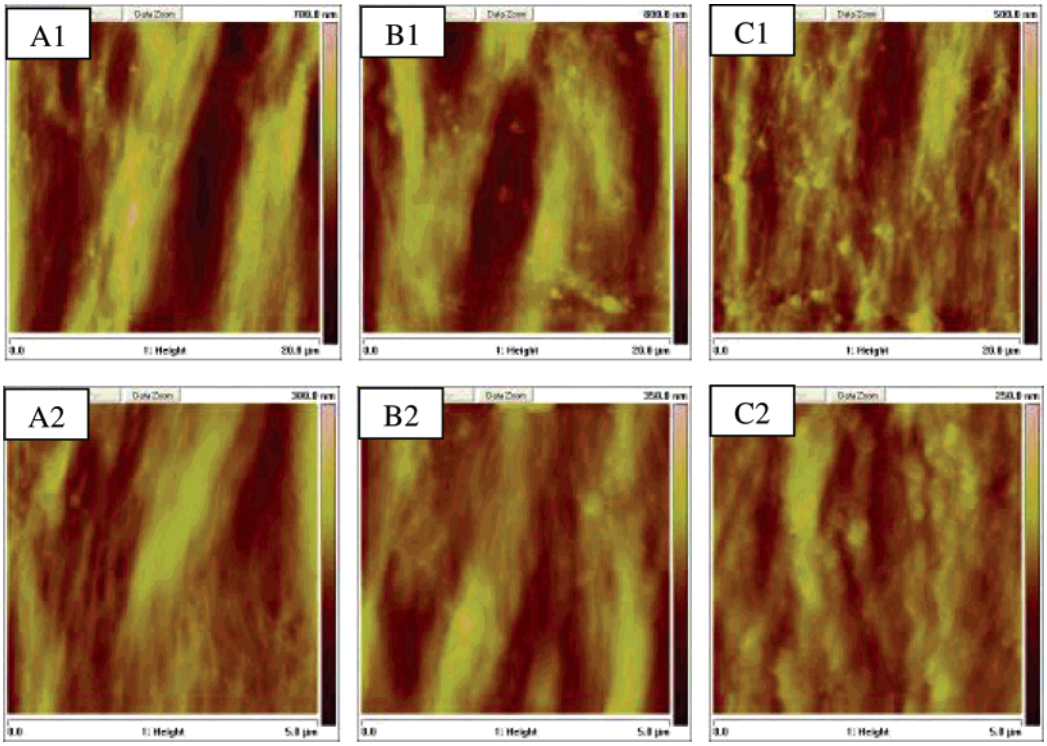

Figure 5. AFM images of the biaxially drawn films of different fabrication methods (A: spin cast; B: 2-roll mill; C: solvent cast) at side region.

of center (1) and side (2). A very dense network of fibrillar structures was observed in all optical images. The orientation of the fibrils at the center regions for all films did not follow a particular orientation. Generally, it was quite isotropic. This was expected as the center region of the film was subjected to near biaxial straining of the fibrils. As compared to the side regions, the fibrils were strongly aligned in a unidirectional manner, as shown in the arrows at the top right corner. This was because the side of the film was subjected to a more unidirectional drawing process. This was also observed in the study of biaxial elongation of semicrystalline poly(ethylene terephthalate) (PET) by Marco et al.[29] A distinct difference in diameters of the fibrils of different fabrication methods was observed. Drawn spin cast film showed a very fine network of fibrils while that of 2-roll mill showed a coarser network. Drawn solvent cast film also showed a network of fibrils intermediate in size. The difference in the size of the fibrils could be due to the different sizes of the spherulites formed at different cooling rates. The spin cast films, which were allowed to evaporate and dry at room conditions, experienced a higher cooling rate than the 2-roll mill and solvent cast films. As a result of fast cooling, the spin cast films had smaller spherulites and the fibrils formed from drawing would thus be significantly thinner.

Uniform biaxially drawn films were achieved with good repeatability using methods of 2-roll mill and solvent casting. Undrawn material was not observed under the microscope, showing that the drawing ratio of both film types were sufficient in transforming the lamellae structures into fibrils. However, for the spin cast films, regions of undrawn materials were found. Figure 4 shows the center region of the biaxially drawn spin cast PCL film with fibrils extending radially outward from the undrawn material. The existence of the undrawn materials could be due to inefficient transfer of the drawing forces to the fibrils as stress transfer over very thin structures is always difficult because of thickness variations.

AFM images of drawn PCL films at the side region are shown in Figure 5 and those in the center region in Figure 6. In Figure 5, all three types of PCL films show a unidirectional alignment of fibrils and are similar to the microstructures as shown previously in Figure 3. The thick rodlike structures shown in Figure 5 A1 and B1 could be the macrofibrils; when scanned at a higher resolution of 5 μm $\times$ 5 μm as shown in A2 and B2,

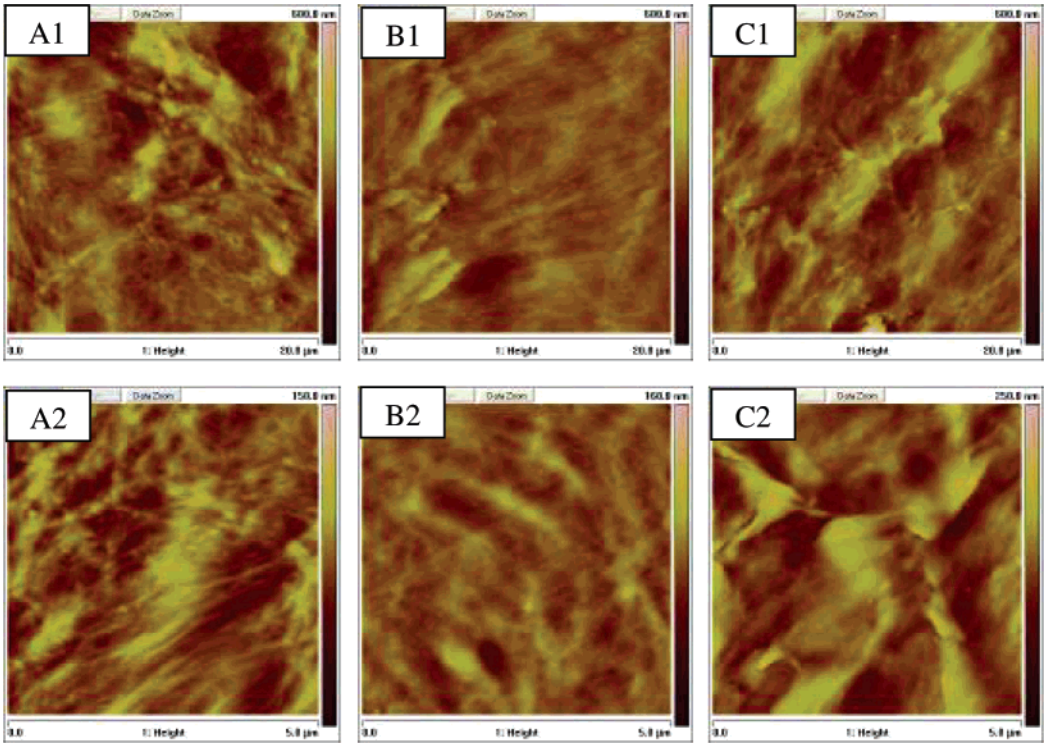

Figure 6. AFM images of the biaxially drawn films of different fabrication methods (A: spin cast; B: 2-roll mill; C: solvent cast) at center region.

the macrofibrils could be seen thinning and slipping away to form microfibrils in a unidirectional orientation.

Figure 6 shows the AFM images in the center regions of the drawn PCL films. Fibrillar networks were observed and the fibrils were also no longer aligned unidirectionally and were seen to be oriented nonpreferentially. These results were in agreement with the images shown by the polarized optical microscopy in Figure 3. However, biaxial or radial alignment of the fibrils was not as obvious as the image shown in Figure 4 where the fibrils were seen extending radially from the undrawn material. This can be explained by the fact that while the biaxial force at the four corners of the film was released after the drawing process, the fibrils experienced a stress relaxation that caused the fibrils to coil back from its biaxially drawn direction. Such relaxation, which can result in shrinkage, was reported by Zhang and Ajji[5] in biaxial drawing of polystyrene.

Thermal Properties of PCL films (DSC). Biaxial drawing produced a significant effect on the melting behavior of the films. This was expected because of structural changes by biaxial drawing, and these were indicated in the melting endotherms in Figure 7 and the melting temperature, enthalpies, and percentage crystallinities in Table 2. Figure 7 shows a series of DSC traces of drawn and nonbiaxially drawn PCL films. The traces showed very well defined profiles of a material with a typical semicrystalline characteristic. The nonbiaxially drawn PCL films melted at temperature of 62.0 °C for spin cast film, 62.2 °C for solvent cast film, and 62.9 °C for 2-roll mill film. All these three types of undrawn films showed similar melting temperature. After biaxial drawing, the melting temperatures of the films were 63.6 °C for spin cast film, 63.3 °C for solvent cast film, and 62.5 °C for 2-roll mill film. No notable change in melting temperatures was observed after 2-roll mill films were drawn. An increase of 1.1 °C was observed in drawn solvent cast film while an increase of 1.6 °C was observed in drawn spin cast film. Increase in melting temperature after biaxial drawing of polymers was also reported elsewhere.[4,7,10] Since melting temperature is dependent on crystallite sizes, the increase in melting temperature suggests the presence of larger, thicker lamellae that were formed during the biaxial drawing at near melting temperature of the PCL.

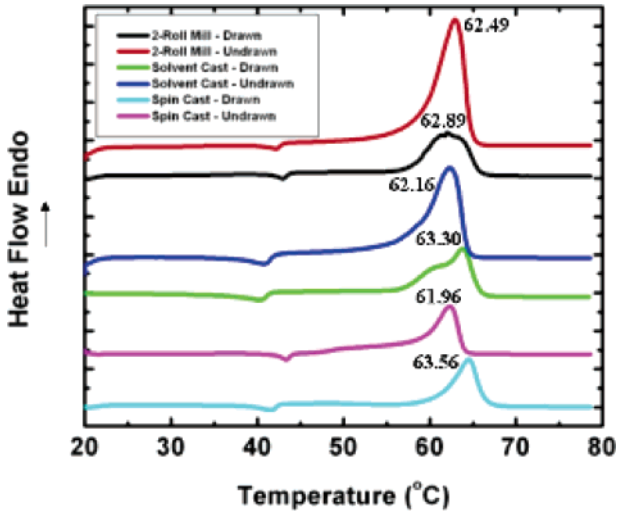

Figure 7. DSC profiles of drawn and undrawn PCL films.

Table 2. Peak Temperatures, Melting Enthalpies, and Percentage Crystallinity of the Drawn and Undrawn PCL Films

film types	peak temp. (°C)	enthalpy (J/g)	% cryst.
Nonbiaxially Drawn Films			
spin cast	62.0	73.8	52.9
2-roll mill	62.9	69.6	49.9
solvent cast	62.2	68.0	48.7
Biaxially Drawn Films			
spin cast	63.6	65.2	46.7
2-roll mill	62.5	65.5	47.0
solvent cast	63.3	62.8	45.0

The melting profiles of the films fabricated by method of solvent casting and 2-roll milling showed a reduction and broadening in the peaks after biaxial drawing, as compared with pointed and narrow peaks before biaxial drawing. The biaxial drawing process broke up the lamellae and widened the lamellae size distribution, which was evident by the broadening of the melting trace since crystallite sizes affect glass-transition temperatures. For spin cast films, the peak remained relatively unchanged after biaxial drawing but a slight shift of the melting peak at higher temperatures was observed.

Table 2 shows the peak temperature, melting enthalpy, and percentage crystallinity of the PCL films. The percentage crystallinity of the film was calculated against the melting enthalpy of 100% crystalline PCL at 139.5 J/g.[23] The degree of crystallinity was observed to be 4−6% lower after biaxial drawing for all three types of films. This indicated the destruction of crystalline material as the large lamellae (folded chain structures) were subjected to drawing to form microfibrils (extended chain structures).

These results appear to be different from the findings by Ng et al.[4] that biaxially drawn film saw an increase in the melting enthalpy. This difference in results could be due to different cooling techniques being adopted. Slow cooling after melt pressing was carried out in this experiment while Ng et al. adopted quenching of melt-pressed films in ice water.

The lamina thickness L is related to cooling rate ΔT[30] by

$$L = \frac{2\sigma_e T_m^{\ O}}{\Delta H_f \Delta T} + \delta L$$

where σ_e, ΔH_f, $T_m^{\ O}$, and δL is the fold surface energy, heat of fusion, equilibrium melting temperature, and a quantity arising from the kinetic theory (which varies slowly with cooling rate), respectively. From the equation, slow cooling produces larger and thicker lamellae while fast cooling like quenching produces smaller and thinner lamellae and lower crystallinity. Smaller lamellae may suggest a more ordered fibrillar structure after biaxial drawing while larger lamellae from slow cooling may produce a less ordered fibrillar structure.

Water Vapor Transmission Rate (WVTR). One of the critical concerns in the search for good tissue engineering scaffolds is the mass transport issue. Cells need supplies of nutrients and other vital substances, such as oxygen, to survive. This transport is accomplished through blood vessels and capillaries in vivo; under in-vitro conditions where the tissue grown is avascular, physical diffusion and permeation are the only possible routes to provide for delivery of these substances. Thus, it is believed that permeable scaffolds are more suitable for healthy tissue growth. As a result, the testing for transport of small molecules, such as water vapor, through the films becomes indispensable in our assessment of the membranes via the water vapor permeability test.

There are possible sources of errors in water vapor permeability tests such as local defects, leakage, resistance to transmission from the still air layer between water surface and film, and resistance of the two surfaces of the film.[31] For permeable thin films, these sources of errors may cause significant differences to the vapor transmission rates measured. In the experiments conducted, leakage was minimized by carefully sealing the opening circumference of the tube using parafilm to prevent vapor from escaping, still air gap between water surface to the film surface was kept at a minimum, and the surfaces of the films were carefully cleaned with ethanol to minimize contamination which could potentially increase surface resistance.

Table 3. Values of Thicknesses and WVTR of Different PCL Films

film type	mean film thickness (μm)	WVTR (g/(h m^2))
free water surface		171.9
biaxially drawn spin cast	1.15	74.96
nonbiaxially drawn spin cast before heat treatment	1.58	67.77
nonbiaxially drawn spin cast after heat treatment	2.68	46.88
biaxially drawn 2-roll mill	10.7	43.10
biaxially drawn solvent cast	14.0	38.24
biaxially drawn 2-roll mill (double layer)	23.67	33.43
biaxially drawn solvent cast film reported by Htay[9]	10.4	30.50

The WVTR test was first performed for four types of PCL films, namely, biaxially drawn 2-roll mill film, solvent cast film, spin cast film, and nonbiaxially drawn spin cast film. The values of the WVTRs obtained are tabulated in Table 3.

It can be seen that the single-layer biaxially drawn solvent cast films had the lowest WVTR at 38.24 g/h m^2 while the biaxially drawn spin cast PCL films had the highest WVTR at 74.96 g/h m^2. The WVTR was 43.10 g/h m^2 for biaxially drawn 2-roll mill films. However, Htay et al.[9] had reported a WVTR of 30.5 g/h m^2 at 10.4 μm for solvent cast microthin PCL films. Judging from the results in Table 3, one would have expected Htay et al.'s films to have a WVTR that was higher than the biaxially drawn solvent cast PCL films or close to the value registered by biaxially drawn 2-roll mill PCL films. One of the reasons for the lower WVTR recorded by Htay et al. could be due to the larger resistance to water vapor transmission caused by the depth of the air gap below the film. In this experiment, the air gap was kept at a minimum to 5 mm as compared to Htay et al.'s 45 mm. This big difference thus played a significant role in the difference recorded. Another reason for such discrepancy would be due to the size of spherulites. In Htay et al.'s experiment, his PCL membranes were subjected to ice water quenching immediately after they were heat-pressed, since his PCL membranes were fabricated in the same manner as described by Ng et al. However, the PCL films tested here were slow-cooled after being melt-pressed. As mentioned previously, slow cooling produces larger and thicker lamellae, and a less ordered fibrillar structure after biaxial drawing while quenching produces smaller and thinner lamellae and a more ordered fibrillar structure after biaxial drawing. As a result, a much more compact and dense structure would be expected in the quenched PCL films, and hence it provided a larger resistance for water molecules to diffuse through, thereby having a WVTR that was significantly lower than the PCL films that were allowed to slow-cool.

An ideal correlation between thickness and WVTR for homogeneous film types is governed by Fick's Law of steady-state transport. Strictly speaking, the wet cup test in accordance to ASTM E96-00 E requires a steady state of water vapor transport to be established across the barrier membrane. For this condition to be achieved, it is required that the relative humidity (RH) levels on both surfaces of the film be maintained constant such that the outside surface facing the air is kept at 50% RH by the humidity chamber and the inner surface facing distilled water is maintained at 100%RH by the evaporation of water.[32]

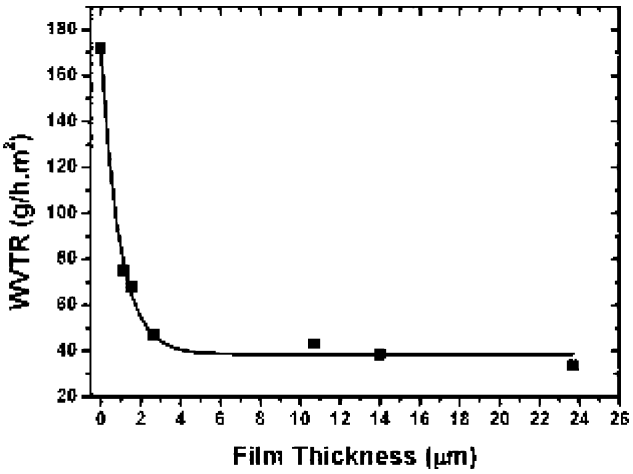

Figure 8. WVTR plotted against film thickness for various film types.

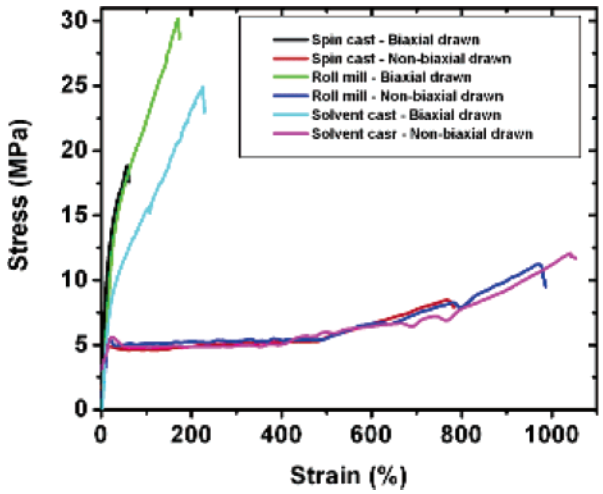

Figure 9. Stress−strain curves of all different PCL films being investigated.

Under this steady-state condition, the transport of water vapor through the film governed by Fick's law of steady-state diffusion[33] can be concisely expressed by the following relation:

$$\text{flux} = -\not{p}\frac{dP}{dx} = \frac{G}{t}$$

where p is the permeability coefficient of the material that depends on material characteristics, and dP/dx is the gradient of the driving force of transport. Under steady state, this gradient would be equal to $\Delta P/l$, where ΔP is the pressure or concentration or potential difference across the film and l is the thickness. Since WVTR is flux divided by the cross-sectional area, it can be deduced that WVTR is proportional to $\Delta P/l$ under steady-state conditions, which leads to the conclusion that WVTR should be inversely proportional to film thickness l if fabrication methods have no influence on the material permeability $\not{p}$.

The WVTR of free water surface was determined at 171.90 g/(h m^2), and this result matches closely to the value of 167.75 g/(h m^2) established,[9] hence verifying the matching accuracy of this test setup. A wide range of film types have been fabricated and used in the test. Stacking of 2-roll mill films was also carried out to explore WVTR at higher thickness. As mentioned earlier, Fick's law states that the WVTR is inversely proportional to the film thickness provided the films are homogeneous. Since the films were fabricated by different techniques, these films could not be considered to be homogeneous. However, judging from the difference between biaxially drawn 2-roll mill film and biaxially drawn solvent cast film by Htay et al., we could allow the values of the WVTR to be plotted against film thickness because error margin caused by the inhomogenity by different film processing techniques accounted for less than 50%. Figure 8 showed the WVTR versus thickness.

It can be seen clearly observed from Figure 8 that an exponential decay between WVTR and film thicknesses can be established. This predicted accurately that WVTR is inversely proportional to its thickness. The relative magnitudes of WVTR values of the available films could be concluded such that biaxially drawn spin cast films always give the highest level of transmission rate compared to all other films, possibly because of their lowest thickness or structural differences. It was also believed that spin cast films have undergone a rather limited amount of drawing such that the fibrillar structure is not fully formed as undrawn materials were observed under the microscope. Drawing defects might have also caused the presence of many microvoids in the structure such that micropores existed to allow the direct flow of water vapor through the membrane instead of diffusion and sorption. Thus, these microvoids had enhanced the transmission rate of water vapor.

Tensile Properties. The stress−strain curves of the PCL films are shown in Figure 9. Distinct differences in the tensile strength and elongation could be seen from the graph upon biaxial drawing of the films. Biaxially drawn films exhibited higher tensile strength while that of nonbiaxially drawn films exhibited greater elongation.

For nonbiaxially drawn films, all three fabrication methods yielded similar tensile characteristics. Yielding took place at a stress of about 5 MPa which was followed by cold drawing till it reached strain of 500%. At this stage of cold drawing, the spherulites were drawn to form macrofibrils, similar to what happened to the PCL structures during biaxial drawing. At strain of 500% and beyond, strain hardening took place. A higher tensile force was required to stretch further the fully extended macrofibrils into microfibrils, and the films finally fractured beyond its tensile strength of 8.2, 11.4, and 10.9 MPa for spin cast, roll mill, and solvent cast films, respectively. Roll mill and solvent cast films had almost the same elongation at break of about 1000% while spin cast films had a lower elongation at break of 720%. The lower tensile strength and elongation for spin cast film were expected because of nonuniform microstructure as compared to the rest of the films and the smaller spherulites formed caused by fast evaporation of solvent.

Upon biaxial drawing, the elongation was reduced to 59.6%, 183.0%, and 229.5% for spin cast, roll mill, and solvent cast films, respectively. The elongation became much smaller as compared to their nonbiaxially drawn counterparts because after biaxial drawing, the microfibrils were almost fully stretched to their limit. At this point when all spherulites had strain-hardened to form microfibrils, elongation became substantially reduced and any force applied was utilized to deform and fracture the microfibrils. Hence, this explained the reduction in the elongation at break. At the same time, the modulus of the films increased because of the strain-hardening stage. The modulus of spin cast films increased by approximately 58% from 223.2 to 352.8 MPa while that of roll mill films increased by about 25% from 273.3 to 339.3 MPa. However, the solvent cast films registered a reduction in modulus from 262.3 to 214.5 MPa. In biaxially drawn films, greater force was required to stretch and deform the strain-hardened microfibrils as compared to nonbiaxially drawn films where less force was required to draw the

Table 4. Values of Modulus (E), Ultimate Tensile Strength σ_{UTS}, and Elongation (λ) of All Types of PCL Films

films types	E (MPa)	σ_{UTS} (MPa)	λ (%)
Nonbiaxially Drawn Films			
spin cast	223.2	8.2	720.6
roll mill	273.3	11.4	978.7
solvent cast	262.3	10.9	1000.6
Biaxially Drawn Films			
spin cast	352.8	20.7	59.6
roll mill	339.3	30.6	183.0
solvent cast	214.5	24.8	229.5

spherulites into macrofibrils. Strain hardening upon biaxial drawing also resulted in the tensile strength of all PCL films to increase by approximately 2.5 folds. The tensile strength of spin cast, roll mill, and solvent cast PCL films increased to 20.7, 30.6, and 24.8 Mpa, respectively. The distinct enhancement in the modulus and tensile strength of the biaxially drawn PCL films could be attributed to the effect of annealing after biaxial drawing whereby the stress imposed on the microfibrils becomes relaxed. As mentioned earlier, the increase in melting temperature after biaxial drawing at near melting temperature and annealing resulted in the growth of thicker lamellae, and this aspect further substantiated the results for the increase in tensile strength and modulus of the films.

Table 4 summarizes the tensile characteristics of all types of PCL films before and after biaxial drawing. Biaxially drawn spin cast films were found to have a higher modulus and were hence stiffer than the other two types of biaxially drawn films. Also, it was found that biaxially drawn spin cast films have the least tensile strength.

Conclusion

Comparative study was carried out for biaxial drawing of films made from 2-roll mill, standard solution casting, and spin casting. The fabrication of sub-micrometer ultrathin PCL films was succefully carried out through biaxial drawing of the spin cast films. All films were biaxially drawn to their limit, and it was found that films made from 2-roll mill have the highest drawing ratio while that of spin cast films have the lowest drawing ratio. The morphology of all the biaxially drawn films studied showed similar fibrillar networks because of chain orientation induced by biaxial drawing. Thermal analysis revealed an increase in the melting peak temperature of the films upon biaxial drawing but a drop in the percentage crystallinity. The WVTR was found to be inversely proportional to film thickness and can be dependent on the effect of quenching. Biaxially drawn spin cast films, being the least thick, therefore have the highest WVTR as compared to the rest of the biaxially drawn films. The mechanical properties determined through tensile test showed that upon biaxial drawing, all films exhibited a reduction in elongation, an increase in tensile strength, and an increase in modulus. However, for solvent cast films, the modulus decreased.

From the results, biaxially drawn 2-roll mill films not only possessed the preferred mechanical properties, they also offered reduced thickness as compared to the solvent cast films because of higher drawing ratio. With their good mechanical properties, they can match the commercially available wound dressings such as Omiderm.[34] However, taking into consideration the benefits of administering less foreign material over a same surface area in vivo coupled with faster degradation, biaxially drawn spin cast films could also prove important in the area of membrane tissue engineering applications where film thickness is a concern. Transport of water vapor was also much faster, and hence it can be deduced that efficient mass transport of ions necessary for cell proliferation and nutrient/waste tranfer can be carried out. Thus, this fabrication method via spin cast coupled with biaxial drawing seemed to offer potential benefits for membrane tissue engineering applications as well.

Acknowledgment. The authors thank Ms. Tan Phay Shing, Eunice from Nano Biomechanics Laboratory for the setup of AFM, Mr. Zhang Yanzhong from Biomechanics Laboratory for the setup of Instron Universal Tensile Tester, Ms. Satinderpal Kaur from Nanobioengineering Laboratory for the use of DSC, and Mr. K. Sivalingam from Engineering Workshop 2 for the setup of electronic length measuring equipment. The authors also thank the staff and graduate and undergraduate students from BIOMAT and DSI for their contributions.

References and Notes

(1) Kalpakjian, S. In *Manufacturing Processes for Engineering Materials*, 3rd ed.; Addison-Wesley: Reading, MA, 1984.
(2) Farag, M. M. In *Polymeric materials and their processing*; Prentice Hall: New York, 1989.
(3) Ashby, M. F.; Jones, D. R. H. In *Engineering materials 1: An introduction to their properties & applications*, 2nd ed.; Butterworth Heinemann, Oxford, 2001.
(4) Ng, C. S.; Teoh, S. H.; Chung, T. S.; Hutmacher, D. W. *Polymer* **2000**, *41*, 5855−5864.
(5) Zhang, X.; Ajji, A. *J. Appl. Polym. Sci.* **2003**, *89*, 487−496.
(6) Savitskii, A. V.; Levin, B. Y.; Demicheva, V. P. *Polym. Sci U.S.S.R.* **1973**, *15*, 1446−1451.
(7) Lüpke, T.; Dunger, S.; Sänze, J.; Radusch, H.-J. *Polymer* **2004**, *45*, 6861−6872.
(8) Tiaw, K. S.; Goh, S. W.; Hong, M. H.; Z. Wang, Z. B.; Lan, B.; Teoh, S. H. *Biomaterials* **2005**, *26*, 763−769.
(9) Htay, A. S.; Teoh, S. H.; Hutmacher, D. W. *J. Biomater. Sci., Polym. Ed.* **2004**, *15*, 683−700.
(10) Sakai, Y.; Miyasaka, K. *Polymer* **1988**, *29*, 1608−1614.
(11) Sakai, Y.; Miyasaka, K. *Polymer* **1990**, *31*, 51−57.
(12) Sakai, Y.; Umetsu, K.; Miyasaka, K. *Polymer* **1993**, *34*, 318−322.
(13) Khan, T. A.; Peh, K. K.; Ch'ng, H. S. *J. Pharm. Pharm. Sci.* **2000**, *3*, 303−311.
(14) Yudanova, T. N.; Reshetov, I. V. *Pharmt. Chem. J.* **2006**, *40*, 85−92.
(15) Ang, L. P. K.; Cheng, Z. Y.; Beuerman, R. W.; Teoh, S. H.; Zhu, X.; Tan, D. T. H. *Invest. Ophthamol. Vis. Sci.* **2006**, *47*, 105−112.
(16) Matsuda, T. *Artif. Organs* **2004**, *28*, 64−71.
(17) Ng, K. W.; Hutmacher, D. W.; Schantz, J. T.; Ng, C. S.; Too, H. P.; Lim, T. C.; Phan, T. P.; Teoh, S. H. *Tissue Eng.* **2001**, *7*, 441−455.
(18) Khor, H. L.; Ng, K. W.; Schantz, J. T.; Phan, T. T.; Lim, T. C.; Teoh, S. H.; Hutmacher, D. W. *Mater Sci. Eng., C* **2002**, *20*, 71−75.
(19) Serrano, M. C.; Pagani, R.; Vallet-Regí, M.; Peña, J.; Rámila, A.; Izquierdo, I.; Portolés, M. T. *Biomaterials* **2004**, *25*, 5603−5611.
(20) Cheng, Z.; Teoh, S. H. *Biomaterials* **2004**, *25*, 1991−2001.
(21) Prucker, O.; Christian, S.; Bock, H.; Rühe, J.; Frank, C. W.; Knoll, W. *Macromol. Chem. Phys.* **1998**, *199*, 1435−1444.
(22) Wang, M.; Zhu, X.; Wang, S.; Zhang, L. *Polymer* **1999**, *40*, 7387−7396.
(23) Crescenzi, V.; Manzini, G.; Calzolari, G.; Borri, C. *Eur. Polym. J.* **1972**, *8*, 449−463.
(24) Ruiz-Cardona, L.; Sanzgiri, Y. D.; Benedetti, L. M.; Stella, V. J.; Topp, E. M. *Biomaterials* **1996**, *17*, 1639−1643.
(25) Persenaire, O.; Alaxandre, M.; Degée, P.; Dubois, P. *Biomacromolecules* **2001**, *2*, 288−294.
(26) Ruseckaite, R. A.; Jiménez, A. *Polm. Degrad. Stab.* **2003**, *81*, 353−358.
(27) Sivalingam, G.; Madras, G. *Polym. Degrad. Stab.* **2003**, *80*, 11−16.

(28) Sivalingam, G.; Karthink, R.; Madras, G. *Polym. Degrad. Stab.* **2004**, *84*, 345−351.
(29) Marco, Y.; Chevalier, L.; Chaouche, M. *Polymer* **2002**, *43*, 6569−6574.
(30) Narh, K. A.; Odell, J. A.; Keller, A.; Fraser, G. V. *J. Mater. Sci.* **1980**, *15*, 2001−2009.
(31) Graves, R. S.; Zarr, R. R. *ASTM Spec. Tech. Publ. 1320* **1977**, *3*, 456.
(32) Hu, Y.; Topolkaraev, V.; Hiltner, A.; Baer, E. *J. Appl. Polym. Sci.* **2001**, *81*, 1624−33.
(33) Cussler, E. L. In *Diffusion: Mass Transfer in Fluid Systems*; Cambridge University Press, New York, 1997.
(34) Shalak, R., Chien, S. In *Handbook of Bioengineering*; McGraw-Hill: New York, 1987.

BM060832A